PHYSICAL REVIEW B

CONDENSED MATTER AND MATERIALS PHYSICS

THIRD SERIES, VOLUME 57, NUMBER 19 **15 MAY 1998-I**

BRIEF REPORTS

Brief Reports are accounts of completed research which, while meeting the usual **Physical Review B** *standards of scientific quality, do not warrant regular articles. A Brief Report may be no longer than four printed pages and must be accompanied by an abstract. The same publication schedule as for regular articles is followed, and page proofs are sent to authors.*

Orthogonal polynomial projectors for the projector augmented wave method of electronic structure calculations

N. A. W. Holzwarth, G. E. Matthews, A. R. Tackett, and R. B. Dunning

Department of Physics, Wake Forest University, Winston-Salem, North Carolina 27109

(Received 8 September 1997; revised manuscript received 14 January 1998)

The projector augmented wave (PAW) method for electronic structure calculations developed by Blöchl [Phys. Rev. B **50**, 17 953 (1994)] has been very successfully used for density functional studies. It has the numerical advantages of pseudopotential techniques while retaining the physics of all-electron formalisms. We describe a method for generating the set of atom-centered projector and basis functions that are needed for the PAW method. This scheme chooses the shapes of the projector functions from a set of orthogonal polynomials multiplied by a localizing weight factor. Numerical benefits of the scheme result from having direct control of the shape of the projector functions and from the use of a simple repulsive local potential term to eliminate ''ghost state'' problems, which can plague calculations of this kind. Electronic density of states results are presented for the mineral powellite ($CaMoO_4$). [S0163-1829(98)03416-X]

I. INTRODUCTION

The projector augmented wave (PAW) method of electronic structure calculations, developed by Blöchl[1] and also used by our group,[2] is a very powerful method for electronic structure calculations within the framework of density functional theory.[3] In order to use this method, it is necessary to find three types of atom-centered functions—''projectors,'' all-electron basis functions, and smooth pseudo basis functions. Schemes for constructing these functions have been discussed in the literature.[1,2,4] Our earlier scheme[2] was found to work well for some materials, but failed for others. We describe a mathematically well-controlled method for generating the projector and basis functions that promises to work very well throughout the Periodic Table.

II. FORMALISM

Following the notation of Refs. 1 and 2, the functions that are needed for each atomic type a are denoted $\{\phi_i^a(\mathbf{r}), \tilde{p}_i^a(\mathbf{r}), \tilde{\phi}_i^a(\mathbf{r})\}$, representing the all-electron (AE) basis functions, the projector functions, and the pseudo (PS) basis functions, respectively. The first step in the process is the solution of the all-electron self-consistent Schrödinger equation for the atom and the selection of the appropriate set of upper core and valence AE basis functions $\{\phi_i^a(\mathbf{r})\}$ having one-electron energies $\{\varepsilon_i^a\}$. The task is then to choose the corresponding projector functions $\{\tilde{p}_i^a(\mathbf{r})\}$ and PS basis functions $\{\tilde{\phi}_i^a(\mathbf{r})\}$, which must satisfy a number of conditions. First, in order to accurately transform between the calculated PS wave functions and their corresponding AE functions, the projectors should approximately satisfy a generalized completeness condition within each atomic sphere of radius r_c^a:

$$\sum_i |\tilde{\phi}_i^a(\mathbf{r})\rangle\langle\tilde{p}_i^a(\mathbf{r}')| \approx \delta(\mathbf{r}-\mathbf{r}') \quad \text{for } r,r' \leq r_c^a . \tag{1}$$

Each projector function must vanish and each PS basis function must become equal to its corresponding AE basis function outside the atomic sphere:

$$\tilde{p}_i^a(\mathbf{r}) = 0 \quad \text{and} \quad \tilde{\phi}_i^a(\mathbf{r}) = \phi_i^a(\mathbf{r}) \quad \text{for } r \geq r_c^a . \tag{2}$$

The projector and PS basis functions must satisfy a generalized orthonormality relation:[1]

$$\int d^3r\, \tilde{\phi}_i^a(\mathbf{r})\tilde{p}_j^a(\mathbf{r}) = \delta_{ij} . \tag{3}$$

In addition, the PS basis functions $\{\tilde{\phi}_i^a(\mathbf{r})\}$ satisfy an atomic PAW Hamiltonian equation of the form[1,2]

$$(\varepsilon_i^a - \widetilde{H}^a)|\widetilde{\phi}_i^a\rangle = \sum_j |\widetilde{p}_j^a\rangle\langle\widetilde{\phi}_j^a|(\varepsilon_i^a - \widetilde{H}^a)|\widetilde{\phi}_i^a\rangle, \quad (4)$$

where the pseudo-Hamiltonian function $\widetilde{H}^a$ has a kinetic energy operator and an effective potential contribution:

$$\widetilde{H}^a(\mathbf{r}) \equiv -\frac{\hbar^2}{2m}\nabla^2 + \widetilde{v}_{\rm eff}^a(r). \quad (5)$$

The effective potential $\widetilde{v}_{\rm eff}^a(r)$ must be determined self-consistently as discussed below.

Since the required functions are constructed from equations for a spherical atom, each of them can be written as a radial function times a spherical harmonic function, such as

$$\phi_i^a(\mathbf{r}) \equiv \phi_{n_i l_i m_i}^a(\mathbf{r}) \equiv \frac{\phi_{n_i l_i}^a(r)}{r} Y_{l_i m_i}(\hat{\mathbf{r}}). \quad (6)$$

Since we can construct the projector and basis functions for a single atom at a time, it will be convenient to suppress the index a from some of the expressions below. We will also suppress the running orbital index i throughout the rest of the manuscript and focus our attention on the radial functions $\{\phi_{nl}^a(r)\}$, $\{\widetilde{\phi}_{nl}^a(r)\}$, and $\{\widetilde{p}_{nl}^a(r)\}$. In general, the index n denotes a principal quantum number corresponding to upper core and valence states, and can also be used to enumerate continuum functions needed to augment the basis.[1,2]

In the present work, we approximate the completeness property (1) by setting the projectors to be equal to a set of weighted orthogonal functions. One convenient set of such functions can be derived from the eigenstates of the Schrödinger equation for the three-dimensional harmonic oscillator:

$$f_{Nl}(r) \equiv \mathcal{N}_{Nl} e^{-r^2/\sigma^2} r^{l+1} F\left(-N, l+\frac{3}{2}, \frac{r^2}{\sigma^2}\right). \quad (7)$$

Here, the parameter σ is chosen so that $f_{Nl}(r > r_c^a) \approx 0$ within a specified tolerance, $\mathcal{N}_{Nl}$ is a normalization constant, and $F(-N, l+3/2, r^2/\sigma^2)$ denotes a confluent hypergeometric function,[5] which is a finite polynomial of order N ($N=0,1$, etc.) in the variable of (r^2/σ^2). Figure 1 shows the shape of some of the functions $f_{Nl}(r)$.

Our ''orthogonal polynomial projector'' formalism thus starts by assuming that each radial projector function is proportional to one of the functions $f_{Nl}(r)$:

$$\widetilde{p}_{nl}^a(r) = \mathcal{A}_{nl} f_{(n-n_0)l}(r), \quad (8)$$

where the amplitude $\mathcal{A}_{nl}$ will be evaluated below and where n_0 corresponds to the first of the chosen AE radial basis functions $\phi_{n_0 l}^a(r)$ for a given l. The following recipe then ensures that the atom-centered radial functions $\{\phi_{nl}^a(r)\}$, $\{\widetilde{\phi}_{nl}^a(r)\}$, and $\{\widetilde{p}_{nl}^a(r)\}$ satisfy the relations 2, 3, and 4.

For each AE radial basis function $\phi_{nl}^a(r)$, we define the corresponding PS radial basis function $\widetilde{\phi}_{nl}^a(r)$ according to

$$\widetilde{\phi}_{nl}^a(r) = \sum_{n'} \mathcal{B}_{nl}^{n'} \chi_{nl}^{n'}(r). \quad (9)$$

The indices n and n' enumerate all the (M_l) basis functions needed for the given orbital quantum number l. Typically,

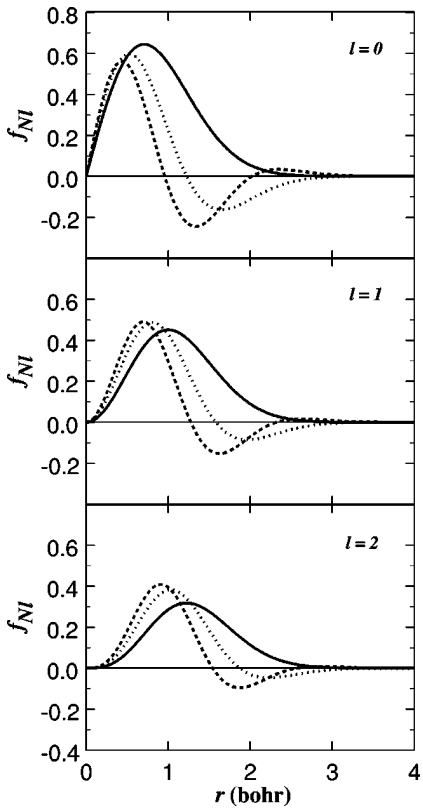

FIG. 1. Plots of the projector basis functions defined in Eq. (7) for $\sigma = 1$ and $N = 0$ (solid line), 1 (dashed line), and 2 (dotted line).

$M_l = 1$ or 2. For each n and n', the functions $\chi_{nl}^{n'}(r)$ are defined to be solutions of inhomogeneous differential equations of the form

$$\left(\varepsilon_{nl}^a - \left[-\frac{\hbar^2}{2m}\frac{d^2}{dr^2} + \widetilde{v}_{\rm eff}^a(r)\right]\right)\chi_{nl}^{n'}(r) = \mathcal{C}_{nl}^{n'} f_{(n'-n_0)l}(r), \quad (10)$$

with the boundary conditions that all of the $\chi_{nl}^{n'}(r)$ functions are continuous at $r=0$. At the atomic sphere radius $r = r_c^a$, they satisfy

$$\chi_{nl}^{n'}(r_c^a) = \phi_{nl}^a(r_c^a) \quad \text{and} \quad \frac{d\chi_{nl}^{n'}(r_c^a)}{dr} = \frac{d\phi_{nl}^a(r_c^a)}{dr}. \quad (11)$$

The differential equation (10) and boundary conditions (11) *uniquely* determine the functions $\chi_{nl}^{n'}(r)$ and the amplitudes $\mathcal{C}_{nl}^{n'}$. A Numerov algorithm[6] for solving these equations is detailed in the Appendix.

Once the solutions $\chi_{nl}^{n'}(r)$ are determined, the M_l expansion coefficients $\mathcal{B}_{nl}^{n'}$ can be calculated from the following linear relations:

$$\sum_{n'} \mathcal{B}_{nl}^{n'} = 1,$$

$$\sum_{n'} \mathcal{B}_{nl}^{n'}\left[\int_0^\infty dr\, \chi_{nl}^{n'}(r) f_{(n''-n_0)l}(r)\right] = 0 \quad \text{for} \quad n'' \neq n. \quad (12)$$

Finally, amplitude factor $\mathcal{A}_{nl}$ can be calculated in terms of the expansion coefficients $\mathcal{B}_{nl}^{n'}$:

$$\mathcal{A}_{nl}=\frac{1}{\Sigma_{n'}\mathcal{B}_{nl}^{n'}[\int_0^\infty dr\,\chi_{nl}^{n'}(r)f_{(n-n_0)l}(r)]}. \tag{13}$$

The projector functions (8) and PS basis functions (9) found in this way satisfy the PAW Hamiltonian equation (4) and also satisfy conditions 2 and 3. The above procedure, solving Eqs. (10), (11), (12), and (13), determines the projector and basis function for a fixed value of the effective potential $\tilde{v}^a_{\rm eff}(r)$. In order to derive the optimal functional forms, these equations should be solved self-consistently, since $\tilde{v}^a_{\rm eff}(r)$ depends upon the basis functions through the corresponding valence PS and AE density functions:

$$\tilde{n}^a(r)=\sum_{nl} w_{nl}\frac{|\tilde{\phi}^a_{nl}(r)|^2}{4\pi r^2} \quad \text{and} \quad n^a(r)=\sum_{nl} w_{nl}\frac{|\phi^a_{nl}(r)|^2}{4\pi r^2}, \tag{14}$$

where $w_{nl}[\leqslant 2(2l+1)]$ denotes the orbital occupation. The smooth effective potential for the atom is given by[1,2]

$$\tilde{v}^a_{\rm eff}(r)=e^2Q^a_{00}\frac{\mathrm{erf}(r/\sigma)}{r}+\tilde{v}^a_{\rm loc}(r)+e^2\int d^3r'\frac{\tilde{n}^a(r')}{|\mathbf{r}'-\mathbf{r}|}+\mu_{xc}[\tilde{n}^a(r)]. \tag{15}$$

Here Q^a_{00} is the compensation charge in terms of the atomic number Z^a, the core electron charge $Q^a_{\rm core}$, and a valence density correction term $Q^a_{00}=-Z^a+Q^a_{\rm core}+\int_{r\leqslant r_c^a}d^3r[n^a(r)-\tilde{n}^a(r)]$. The self-consistent scheme to determine the PS basis functions $\{\tilde{\phi}^a_{nl}(r)\}$ can be thought of as a constrained minimization of the PS energy functional $\tilde{E}$ defined by Blöchl.[1] For each atom, the shape of the projector and basis functions depends on the choice of the matching radius r_c^a, of the Gaussian length parameter σ, and of the form of $\tilde{v}^a_{\rm loc}(r)$. Typically, we choose σ such that $e^{-(r_c^a/\sigma)^2}\leqslant 10^{-6}$.

The localized potential term that appears in Eq. (16) vanishes for $r>r_c^a$. In the current scheme, the form of $\tilde{v}^a_{\rm loc}(r)$ is arbitrary and can be used to optimize the PAW calculation. A convenient form is given by

$$\tilde{v}^a_{\rm loc}(r)=V_0e^{-r^2/\sigma^2}, \tag{16}$$

where V_0 is an adjustable parameter. Preliminary indications are that it is possible to get good results for many materials (for example, C, O, F, Ca, and Si) using $V_0\equiv 0$. However, since the PAW formulation uses a separable potential it sometimes suffers from the well-documented phenomenon of ''ghost'' states.[7] We examined two systems (Fe and Mo) that exhibited this ghost state behavior and, for both of them, we were able to eliminate the problem by introducing a repulsive local potential $\tilde{v}^a_{\rm loc}$ with a large enough amplitude ($V_0>0$). Gonze and co-workers[7] studied the mathematical origin of these unphysical states and found that they are more likely to occur when there exist eigenstates of the ''local'' Hamiltonian ($\tilde{H}^{\rm PW}$ in the notation of Blöchl[1]) below the physical eigenstates of the system. In the PAW approach, the potential due to the ''compensation'' charge density $\hat{n}(r)$ is usually attractive and thus can shift the eigenvalue spectrum of $\tilde{H}^{\rm PW}$ toward negative values. Therefore, introducing a repulsive localized potential [Eq. (16) with $V_0>0$] can shift the eigenvalue spectrum of $\tilde{H}^{\rm PW}$ to higher energy values. Of course, the contributions of both $\hat{n}$ and of $\tilde{v}_{\rm loc}$ cancel out in the final result of a well-converged and ghostless calculation.

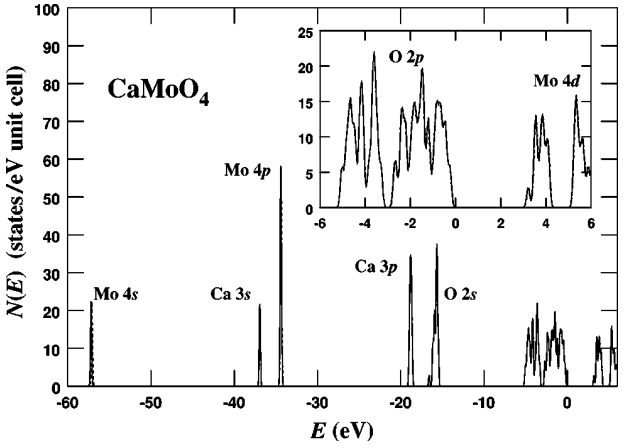

FIG. 2. Plot of the density of states for $CaMoO_4$, $N(E)$ (states/eV/unit cell) calculated using the PAW method (full line) and the LAPW method (dashed line), with the zero of energy taken at the top of the valence band. For both calculations, $N(E)$ was approximated by a weighted sum of Gaussian functions, of width 0.1 eV, centered at each of the energy bands calculated at the 3 sampling k points. The inset shows the bands near the band gap on an expanded scale. The labels indicate the dominant atomic character of each of the bands.

III. RESULTS FOR EXAMPLE SYSTEMS

We have tested this scheme for a few solid state systems– CaF_2, Mo, and the mineral $CaMoO_4$. For CaF_2, results were obtained by generating the projector and basis functions corresponding to neutral F atoms with $r_c^{\rm F}=1.8$ bohr and either neutral Ca atoms or doubly charged Ca^{++} ions with $r_c^{\rm Ca}=2.5$ bohr and 0 values for $V_0^{\rm F}$ and $V_0^{\rm Ca}$. Using a plane-wave cutoff of $|\mathbf{k}+\mathbf{G}|\leqslant 10$ bohr^{-1}, we obtained results for the cohesive energies differing by 0.01 eV/atom, the equilibrium lattice constants differing by 0.002 Å, and the bulk moduli differing by 0.2 GPa compared with each other and with the results of our previous work.[2] For the body-centered cubic metal Mo, results were obtained using $r_c^{\rm Mo}=1.6$ bohr with $V_0=100$ or 500 Ry. Using a plane-wave cutoff of $|\mathbf{k}+\mathbf{G}|\leqslant 13$ bohr^{-1}, we obtained results for the cohesive energies differing by 0.04 eV, the equilibrium lattice constants differing by 0.002 eV, and the bulk moduli differing by 0.8 GPa for the two different choices of V_0.[9]

Calcium molybdate (also known by its mineral name ''powellite'') has been studied since the early 1900s for its very interesting luminescence and structural properties. As part of a study of the electronic structure of this and related materials,[10] we have calculated the density of states for the upper core, valence band, and conduction bands. The $CaMoO_4$ crystal has a tetragonal structure with two formula units (12 atoms) per primitive unit cell. The crystal parameters for the calculation were taken from the experimental neutron analysis.[11] The projector and basis function parameters were similar to those used for our calculations of CaF_2 and body-centered cubic Mo, choosing the local potential parameters for Ca and O to be zero and $V_0^{\rm Mo}=200$ Ry. (Cal-

culations performed with $V_0^{\mathrm{Mo}}=100$ Ry developed ghost states after a few iterations.) The results were obtained using a uniform sampling of the Brillouin zone with three nonequivalent **k** points with a Gaussian weighting scheme[8] and the plane-wave cutoff of $|\mathbf{k}+\mathbf{G}|\leqslant 10$ bohr^{-1}. For comparison, we also performed a calculation using the linear combination of atomic orbital (LAPW) method,[12] using the same **k**-point sampling; muffin-tin radii of 2.0, 1.65, and 1.65 bohr for Ca, Mo, and O, respectively; and using the plane-wave cutoff of $|\mathbf{k}+\mathbf{G}|\leqslant 6$ bohr^{-1}.

For both calculations, $N(E)$ was approximated by a weighted sum of Gaussian functions of width 0.1 eV, centered at each of the energy bands, calculated at the three sampling k points. The results are shown in Fig. 2, with the zero of energy taken at the top of the valence band. What is remarkable about this figure, is that *the two results are virtually indistinguishable* on both the 66 eV range showing the upper core states and on the 12-eV range showing the bands near the band gap. The fact the two independent calculations can achieve such detailed agreement is a testimony to the accuracy of both methods. Further analysis with a better k-point sampling and the inclusion of relativistic effects will be considered elsewhere.[10]

ACKNOWLEDGMENTS

This project was supported by NSF Grant Nos. DMR-9403009 and DMR-9706575. We would also like to thank Peter Blöchl for helpful discussions about the PAW method, R. T. Williams for helpful discussions about $CaMoO_4$, and Yaochun Zhang for help with LAPW calculations on $CaMoO_4$.

APPENDIX: NUMEROV ALGORITHM FOR SOLVING RADIAL DIFFERENTIAL EQUATIONS

Equation (10) which we must evaluate numerically can be written as

$$\frac{d^2\chi(r)}{dr^2}-G(r)\chi(r)=\mathcal{C}F(r), \tag{A1}$$

where we have suppressed all subscripts and superscripts and defined $F(r)\equiv(2m/\hbar^2)f(r)$ and $G(r)\equiv l(l+1)/r^2+(2m/\hbar^2)[\tilde{v}_{\mathrm{eff}}(r)-\varepsilon]$. The Numerov method[6] is most easily applied to a uniform discretization of the functions. Letting Δ denote the radial step size, we can write $\chi_k\equiv\chi(r=k\Delta)$, with $r_c\equiv n\Delta$. It is convenient to replace the continuity of the function and its first derivative boundary condition (11) by requiring that $\chi(k\Delta)=\phi(k\Delta)$ for two consecutive points: $\chi_n=\phi_n$ and $\chi_{n+1}=\phi_{n+1}$. The discretization of Eq. (A1) then becomes a set of n linear equations for n unknowns: $\{\chi_k$, for $k=1,2,\ldots,n-1\}$ and $\mathcal{C}$. These equations can be written in the following matrix form:

$$\begin{pmatrix} b_1 & c_1 & 0 & \ldots & 0 & 0 & -d_1 \\ a_2 & b_2 & c_2 & \ldots & 0 & 0 & -d_2 \\ 0 & a_3 & b_3 & \ldots & 0 & 0 & -d_3 \\ \vdots & \vdots & \vdots & \vdots & \vdots & \vdots & \vdots \\ 0 & 0 & 0 & \ldots & b_{n-2} & c_{n-2} & -d_{n-2} \\ 0 & 0 & 0 & \ldots & a_{n-1} & b_{n-1} & -d_{n-1} \\ 0 & 0 & 0 & \ldots & 0 & a_n & -d_n \end{pmatrix} \begin{pmatrix} \chi_1 \\ \chi_2 \\ \chi_3 \\ \vdots \\ \chi_{n-2} \\ \chi_{n-1} \\ \mathcal{C} \end{pmatrix} = \begin{pmatrix} 0 \\ 0 \\ 0 \\ \vdots \\ 0 \\ -c_{n-1}\phi_n \\ -b_n\phi_n-c_n\phi_{n+1} \end{pmatrix}. \tag{A2}$$

In these equations, the coefficients are defined according to $a_k\equiv 1-(\Delta^2/12)G_{k-1}$, $b_k\equiv -2-(10\Delta^2/12)G_k$, $c_k\equiv 1-(\Delta^2/12)G_{k+1}$, and $d_k\equiv(\Delta^2/12)(F_{k-1}+10F_k+F_{k+1})$. For $l=1$, some of the coefficients must be corrected for the behavior of the equation at $r=0$: $b_1\rightarrow b_1-1/X$ and $d_1\rightarrow d_1-U/X$, where $X\equiv 6\{1+(2m/\hbar^2)[\tilde{v}_{\mathrm{eff}}(0)-\varepsilon]\Delta^2/10\}$ and $U\equiv(2m/\hbar^2)(\Delta^4/10)\lim_{r\rightarrow 0}[f(r)/r^2]$.

[1] P. E. Blöchl, Phys. Rev. B **50**, 17953 (1994).
[2] N. A. W. Holzwarth, G. E. Matthews, R. B. Dunning, A. R. Tackett, and Y. Zeng, Phys. Rev. B **55**, 2005 (1997).
[3] P. Hohenberg and W. Kohn, Phys. Rev. **136**, B864 (1964); W. Kohn and L. J. Sham, Phys. Rev. **140**, A1133 (1965).
[4] Chris B. Van de Walle and P. E. Blöchl, Phys. Rev. B **47**, 4244 (1993).
[5] *Handbook of Mathematical Functions*, edited by Milton Abramowitz and Irene A. Stegun (Dover, New York, 1965), Chap. 13.
[6] Douglas R. Hartree, *The Calculation of Atomic Structures* (Wiley, New York, 1957), p. 71.
[7] Xavier Gonze, Roland Stumpf, and Matthias Scheffler, Phys. Rev. B **44**, 8503 (1991).
[8] C.-L. Fu and K.-M. Ho, Phys. Rev. B **28**, 5480 (1983).
[9] By choosing a larger value of r_c^{Mo} or by relaxing the error tolerance we could have reduced the plane-wave cutoff significantly.
[10] Y. Zhang, N. A. W. Holzwarth, and R. T. Williams, Phys. Rev. B (to be published).
[11] Erdogan Gürmen, Eugene Daniels, and J. S. King, J. Chem. Phys. **55**, 1093 (1971).
[12] P. Blaha and K. Schwarz, and J. Luitz, WIEN97, Vienna University of Technology 1997. [Improved and updated Unix version of the original copyrighted WIEN code, which was published by P. Blaha, K. Schwarz, P. Sorantin, and S. B. Trickey, in Comput. Phys. Commun. **59**, 399 (1990)].